Am J Cancer Res 2026;16(2):623-638
www.ajcr.us /ISSN:2156-6976/ajcr0167827

Original Article

MicroRNA-mediated MAPK signaling promotes isoliensinine-induced apoptosis in oral squamous cell carcinoma via the ROS-dependent mitochondrial pathway and G2 phase arrest

Zi-Wei Cai[1,2*], Wei Zhao[1*], Yu-Ping Gong[3*], Yi-Chuan Zhou[4], Shi-Qi Pu[4], Xiao-Yu Bai[3], Jia-Qi Li[5], Jia Chen[5], Yi-Yuan Bi[5], Yang Wan[1], Yu He[6], Ping Yang[1,7], Min-Hui Li[1,8]

[1]School of Basic Medicine, Chengdu Medical College, Chengdu 610500, Sichuan, China; [2]Clinical Laboratory, Chengdu Xindu District People's Hospital, Chengdu 610500, Sichuan, China; [3]School of Bioscience and Technology, Chengdu Medical College, Chengdu 610500, Sichuan, China; [4]School of Laboratory Medicine, Chengdu Medical College, Chengdu 610500, Sichuan, China; [5]School of Clinical Medicine, Chengdu Medical College, Chengdu 610500, Sichuan, China; [6]Department of Oncology, Nanbu People's Hospital, Nanchong 637300, Sichuan, China; [7]Academic Office, Chengdu Medical College, Chengdu 610500, Sichuan, China; [8]Center of Scientific Research and Experiment, Chengdu Medical College, Chengdu 610500, Sichuan, China. [*]Equal contributors and co-first authors.

Received July 31, 2025; Accepted February 10, 2026; Epub February 15, 2026; Published February 28, 2026

Abstract: Oral squamous cell carcinoma (OSCC) is a common malignancy. Isoliensinine, a bisbenzylisoquinoline alkaloid from *Nelumbo nucifera Gaertn*, exhibits diverse biological activities, but its microRNA-mediated regulation of the MAPK pathway in anti-OSCC remains unreported. Therefore, this study took OSCC cell lines HSC-3 and HSC-4 as research objects to explore the biological activity and the molecular mechanism of isoliensinine on OSCC. The CCK-8 results revealed that isoliensinine inhibited the proliferation of HSC-3 and HSC-4 cells in a time and drug concentration-dependent manner. Analysis of mRNA and small RNA sequencing revealed that isoliensinine induced significant differences in the expression of 1878 genes and 77 microRNAs (miRNAs) in HSC-3 cells. The GO and KEGG analyses of these differentially expressed genes and miRNAs unveiled their potential role in modulating MAPK signaling. Flow cytometry analysis demonstrated that isoliensinine significantly increased reactive oxygen species (ROS) levels, reduced mitochondrial membrane potential (MMP), induced apoptosis, and caused G2 phase arrest in HSC-3 and HSC-4 cells. Western blot results indicated that isoliensinine upregulated the expression of p-p38, p-SAPK/JNK, p-cdc2, p-cdc25C, Bax, cleaved caspase-9/-3, and cleaved PARP, and downregulated the expression of p-ERK1/2, Bcl-2, and Cyclin B1 in HSC-3 and HSC-4 cells. The results demonstrate that isoliensinine induces apoptosis in OSCC cells via ROS-mediated mitochondrial pathways and cell cycle arrest, a process associated with MAPK signaling pathway activation. Transcriptome analysis further revealed that isoliensinine modulates multiple miRNAs that target the MAPK pathway, suggesting that miRNA regulation may mediate its activation of MAPK signaling.

Keywords: Isoliensinine, oral squamous cell carcinoma, MAPK signaling pathway, reactive oxygen species, MicroRNA, apoptosis

Introduction

Oral cancer is a common malignant tumor. According to Global Cancer Statistics 2022, new cases of and deaths from oral cancer are increasing [1]. Oral squamous cell carcinoma (OSCC) counts for approximately 90% of all types of oral cancer and is classified as one of the most invasive malignant tumors due to its high incidence, metastasis, recurrence, and mortality rates [2]. The survival rate of OSCC patients is largely dependent on the clinical stage. According to the statistics of the US National Institutes of Health [3], the five-year relative survival rate for oral cancer patients whose tumors are confined to the primary site at diagnosis is approximately 88.4%, whereas the five-year relative survival rates of oral can-

https://doi.org/10.62347/EXLM2023

cer patients whose tumors have regional lymph node metastasis or distal metastasis at diagnosis have decreased to 69.4% and 36.9%, respectively. Worryingly, the proportion of oral cancer patients who were found to have regional lymph node metastasis or distal metastasis at diagnosis was approximately 67%.

Surgery is one of the selectable treatment modalities for OSCC [4]. However, incomplete resection and the size of the resection margins have the potential to increase the recurrence rate of OSCC, and subsequently diminish patient survival rates [5]. To improve patient survival rates, adjuvant radiotherapy or chemotherapy is often administered after surgery. Among these options, antitumor drugs have received widespread attention due to their diverse antitumor activities and their potential to enhance the efficacy of surgery or radiotherapy as adjunctive treatment options [6]. A retrospective study found that simultaneous radiotherapy and chemotherapy increased overall survival by approximately 20% compared with radiotherapy alone [7]. Regrettably, commonly used anti-OSCC drugs, such as *5-fluorouracil* and *cisplatin*, face the issue of tumor resistance, which greatly reduces the therapeutic efficacy of anti-tumor drugs [8]. It is urgently necessary to find novel and effective active drugs for the therapy for OSCC. Compounds from edible plants, which are characterized by diverse biological activities, low side effects, and easy accessibility, are excellent candidates for clinical antitumor drugs [9].

Many natural alkaloids, such as *Paclitaxel*, *Vincristine,* and *Berberine* have been developed and successfully used in clinical therapy [10]. According to the basic structure of alkaloids, they can be subdivided into several categories, among which the isoquinoline alkaloids are the most common. Isoliensinine is a bisbenzyl-isoquinoline alkaloid extracted from the green germ of mature seeds of *Nelumbo Nucifera Gaertn*. It is considered a highly promising natural compound with various biological activities, such as cardiac arrhythmia prevention, blood vessel protection, and antitumor effects [11]. Notably, isoliensinine has been shown to inhibit the proliferation of various tumor cells, including hepatocellular carcinoma, cervical carcinoma, and breast cancer cells by modulating nuclear factor kappa-B (NF-κB) signaling [12], the protein kinase B (AKT) pathway [13], the p38 kinase (p38) pathway and the stress-activated protein kinase (SAPK)/c-Jun N-terminal kinase (JNK) pathway [14]. However, the molecular mechanism which isoliensinine induces tumor cell death through the regulation of miRNA expression and extracellular signal-related kinase (ERK) signaling has not been studied.

Given that the anti-proliferative effects of isoliensinine on OSCC cells and its underlying molecular mechanisms remain unexplored, this study investigated its biological activity using two established OSCC cell lines (HSC-3 and HSC-4) as model systems. Additionally, this study systematically investigated the molecular mechanisms underlying the anti-OSCC effects of isoliensinine, with a particular focus on its ability to modulate miRNA expression and MAPK (including ERK/MAPK) signaling pathways. The findings of this study provide novel insights into the biological activity and antitumor mechanisms of isoliensinine, potentially facilitating its development as a natural therapeutic agent against OSCC and offering critical knowledge for its potential clinical translation and rational development of derivative compounds with improved antitumor properties.

Materials and methods

Materials

High-sugar DMEM and fetal bovine serum (FBS) were obtained from Gibco (USA). A Cell Counting kit-8 (CCK-8) and a reactive oxygen species (ROS) assay kit- for photooxidation-resistant DCFH-DA were obtained from Dojindo (Japan). A cell cycle and apoptosis analysis kit, an annexin V-fluorescein isothiocyanate (FITC)/propidium iodide (PI) apoptosis detection kit, a mitochondrial membrane potential (MMP) assay kit with JC-1, and RIPA lysis buffer were obtained from Beyotime Biotechnology (China). ProteinSafe™ phosphatase inhibitor cocktail and ProteinSafe™ protease inhibitor cocktail (EDTA-free) were obtained from TransGen Biotech (China). A BCA protein quantification kit was obtained from Vazyme (China). BSA albumin fraction V was obtained from Biosharp (China). Supersensitive ECL kit and RNA extraction reagent were purchased from Oriscience (China). The rabbit antibodies against cle-

aved caspase-9 (#9505), cleaved caspase-3 (#9664), cleaved PARP (#5625), Bax (#5023), Bcl-2 (#3498), p-SAPK/JNK (#4668), p-ERK1/2 (#4370), p-p38 MAPK (#4511), p-cdc25C (#4901), p-cdc2 (#4539), Cyclin B1 (#4138), cdc25C (#4688), cdc2 (#28439), SAPK/JNK (#67096), ERK1/2 (#4695), p38 MAPK (#8690) and GAPDH (#5174), and the HRP-conjugated goat anti-rabbit antibody (#7074) were obtained from CST (USA). All the other chemicals were of analytical grade.

Isoliensinine was obtained from Must Biotechnology (China) and had a purity of 99.58% (Lot: MUST-21042010). Isoliensinine was completely dissolved in dimethyl sulfoxide (DMSO) and stored at -80°C.

Cell culture

The human OSCC cell lines HSC-3 and HSC-4, which have undergone STR authentication, were donated by Professor Mingbo Wu from the State Key Laboratory of Biotherapy of Sichuan University (China) and cryopreserved in a liquid nitrogen container. In accordance with the culture method recommended by the JCRB Cell Bank, HSC-3 and HSC-4 cells were cultured in high-sugar DMEM medium containing 10% FBS at 37°C with 5% CO_2. Cells growing in the logarithmic growth stage were used for subsequent experiments.

Cell viability analysis

HSC-3 and HSC-4 cells were inoculated in 96-well cell culture plates at the same density. Following overnight incubation, isoliensinine at efficacy concentrations of 0, 10, 15, 20, 30, 40, 60, and 80 μM was added for 24 h and 48 h. Then, CCK-8 was added to each sample, and the mixture was incubated for another 2 h. A multimode plate reader (PerkinElmer VICTOR Nivo, USA) was used to measure the absorbance of each well at 450 nm. GraphPad Prism 10.0 software was used to generate the growth inhibition curves of cells after treatment with isoliensinine and to calculate the half-maximal inhibitory concentration (IC_{50}).

Cell cycle assay

After being treated with 0, 20, 40, or 80 μM isoliensinine for 12 h, the HSC-3 and HSC-4 cells were collected and resuspended in 300 μL of precooled PBS. Then, 700 μL of precooled anhydrous ethanol was added, and the mixture was fixed at 4°C overnight. The ethanol was removed by centrifugation, and the cells were resuspended in staining buffer containing RNase-A and PI according to the kit instructions. Then, after being stained in the dark for 30 min, the cells were washed and resuspended in PBS. The cell cycle distribution was subsequently measured and analyzed by flow cytometry (FCM) (ACEA Biosciences NovoCyte Quanteon, USA).

Apoptosis assay

After being treated with isoliensinine for 24 h, HSC-3 and HSC-4 cells were collected and placed in staining buffer containing Annexin V-FITC and PI according to the kit instructions. After staining in the dark for 20 min, the proportion of apoptotic cells was detected and analyzed via FCM.

Mitochondrial membrane potential assay

For the above methods, HSC-3 and HSC-4 cells were resuspended in staining buffer containing a JC-1 fluorescent probe according to the kit instructions. After staining in the dark for 20 min at 37°C with 5% CO_2, the proportion of cells whose red fluorescence shifted to green was detected by FCM to reflect changes of the MMP.

Reactive oxygen species analysis

After treatment with isoliensinine for 12 h, the HSC-3 and HSC-4 cells were collected via digestion and placed in staining buffer containing photooxidation-resistant DCFH-DA dye. After being stained in the dark for 30 min at 37°C, the change in ROS induced by isoliensinine was analyzed via FCM.

RNA sequencing analysis

HSC-3 cells were selected for RNA sequencing (RNA-seq) analysis on the basis of the CCK-8 results. After the isoliensinine treatment for 12 h, the HSC-3 cells were collected and 1 mL of RNA extraction reagent was added to blow the cells repeatedly to ensure that the cells were sufficiently lysed and released the RNA. The lysate was transferred into a cell-freezing tube and snap-frozen in liquid nitrogen for 30 minutes. Then, the tube was transferred to -80°C

for storage. Under dry ice, the prepared RNA samples were sent to Shanghai Majorbio Bio-Pharm Technology Co., Ltd. (https://www.majorbio.com/) for RNA extraction, quality detection, and RNA-seq analysis utilizing the Illumina NovaSeq 6000 sequencing platform and fastp software. Subsequently, gene alignment was conducted in the ensemble database (http://asia.ensembl.org/Homo_sapiens/Info/Index) by HISAT2 software. Furthermore, RSEM software was performed to analyze gene and transcript expression levels. The differentially expressed genes identified through screening were subjected to systematic functional annotation and pathway enrichment analysis. GO (Gene Ontology) functional annotation was performed using the Blastgo software, which categorizes and annotates the DEGs across three dimensions - molecular function, cellular component, and biological process - and reveals their potential biological functional characteristics. KEGG (Kyoto Encyclopedia of Genes and Genomes) pathway enrichment analysis was implemented via the SciPy library in Python, identifying significantly enriched metabolic pathways and signaling networks through hypergeometric distribution tests. All analysis results were based on a significance threshold of $P < 0.05$ to ensure the statistical reliability of the data.

Western blot analysis

After being treated with isoliensinine for 24 h, HSC-3 and HSC-4 cells were dissolved in RIPA lysis buffer containing protease and phosphatase inhibitors, and the cell lysates were centrifuged at 13, 000×g for 20 min at 4°C. The BCA method was used to measure the protein concentration. Following the standardization of protein volume and concentration, 50 μg of total protein was fractionated via 12% sodium dodecyl sulfate-polyacrylamide gel electrophoresis (SDS-PAGE). The proteins were subsequently transferred to polyvinylidene fluoride (PVDF) membranes via electrotransfer at 250 mA. The membranes were blocked for 1 h with 5% BSA at 37°C and incubated overnight at 4°C with the respective primary antibodies, followed by incubation with a secondary antibody conjugated to horseradish peroxidase (HRP) for 2 h. The blots were visualized with a supersensitive ECL chemiluminescence substrate, an enhanced chemiluminescence system (Bio-Rad ChemiDocXRS, USA), and image-lab image acquisition software. The integrated optical density (IOD) values of the protein bands were analyzed via ImageJ analysis software. The relative expression levels of target proteins were expressed as the ratio of their IOD values to the IOD value of the reference protein GAPDH. Phosphorylation levels of proteins were determined by calculating the IOD ratio of the phosphorylated form to the corresponding total protein form.

Statistical analysis

GraphPad Prism 10.0 software was applied for statistical analysis. Each group of experiments was independently repeated three times, and the experimental results are expressed as the means ± standard deviations. Differences between multiple groups were compared by one-way ANOVA and Dunnett's test. Compared with the control group, $P < 0.05$ was considered statistically significant.

Results

Isoliensinine inhibits OSCC cell proliferation

CCK-8 assays demonstrated that isoliensinine inhibited the proliferation of HSC-3 and HSC-4 cells in time- and dose-dependent manners (**Figure 1**). The calculated IC_{50} values revealed differential sensitivity between the cell lines, with HSC-3 cells showing greater susceptibility (24 h: 39.50 μM, $R^2 = 0.9112$; 48 h: 21.10 μM, $R^2 = 0.9903$) compared to HSC-4 cells (24 h: 57.28 μM, $R^2 = 0.9470$; 48 h: 43.31 μM, $R^2 = 0.9842$).

Isoliensinine modulates differentially expressed genes (DEGs) in HSC-3 cells

The inhibitory effect of isoliensinine on cell proliferation was more obvious in HSC-3 cells than in HSC-4 cells. Therefore, HSC-3 cells were selected as the target for mRNA sequencing analysis. The DEGs were analyzed by DESeq2 software with Benjamini-Hochberg (BH) correction and a threshold set at $|\log_2 FC| \geq 1$ and $Padj < 0.05$. The results revealed significant alterations in the expression of 1,878 genes in HSC-3 cells following isoliensinine treatment, with 657 genes being upregulated and 1,221 downregulated. To visualize the analysis results, clustering heatmaps were drawn (**Figure 2A**). Clustering analysis was performed on the basis

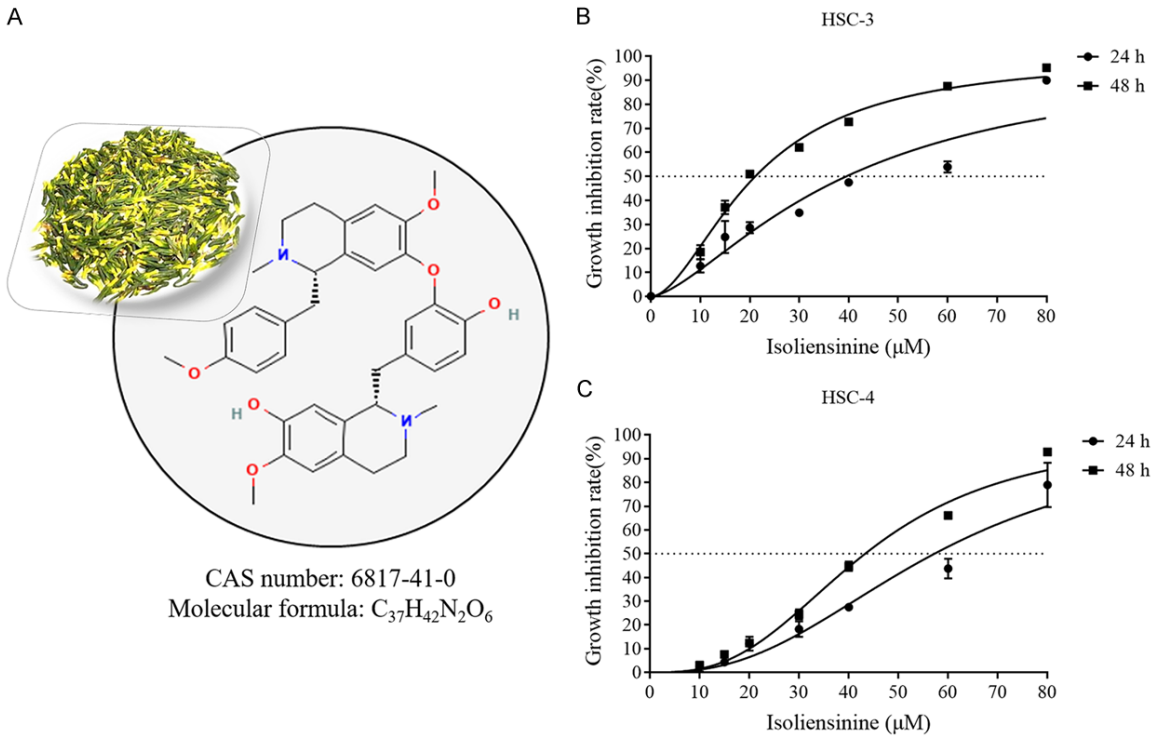

Figure 1. The inhibitory effect of isoliensinine on OSCC cell proliferation. The chemical structure of isoliensinine (A). Growth inhibition curves of HSC-3 cells (B) and HSC-4 cells (C) after treatment with isoliensinine for 24 h and 48 h. Data points represent experimental results from three independent biological replicates (mean ± SD), with curves fitted using a four-parameter logistic model.

of the similarity of gene expression patterns, where genes with similar expression patterns were grouped closer together on the left branch, often indicating functional relevance.

To investigate the effects of isoliensinine on the biological functions and signaling pathways of HSC-3 cells, GO functional annotation analysis and KEGG functional enrichment analysis were performed on the DEGs. GO analysis indicated that the DEGs were related to cellular transcription regulatory activity, membrane part, and response to stimulus (**Figure 2B**). The KEGG analysis indicated that the DEGs may regulate signaling pathways such as p53, MAPK, and PI3K-AKT pathways; cell cycle; apoptosis; and miRNA expression in cancer (**Figure 2C**).

Isoliensinine regulates miRNA differential expression

The KEGG analysis of DEGs induced by isoliensinine in HSC-3 cells revealed that isoliensinine might influence miRNA expression in cancer. Based on the above information, a small RNA-seq analysis was conducted. Differentially expressed miRNAs (DEMs) were analyzed using DESeq2 software with BH correction, applying a significance threshold of *Padj* < 0.05. The results revealed that isoliensinine induced significant expression differences in 77 known and novel miRNAs in HSC-3 cells, with 43 upregulated and 34 downregulated (**Figure 3A**). To comprehensively analyze the potential biological functions of the DEMs, the GO and KEGG databases were used to systematically annotate the predicted target genes and perform pathway enrichment analysis. The GO analysis revealed that these genes were associated with cellular transcription regulatory activity, membrane part, and response to stimulus (**Figure 3B**). KEGG analysis indicated that these genes may regulate signaling pathways such as the cAMP, MAPK, and TNF pathways (**Figure 3C**).

Isoliensinine regulates the MAPK signaling pathway in OSCC cells

KEGG enrichment analysis revealed that the DEGs and DEMs induced by isoliensinine in HSC-3 cells were significantly enriched in the

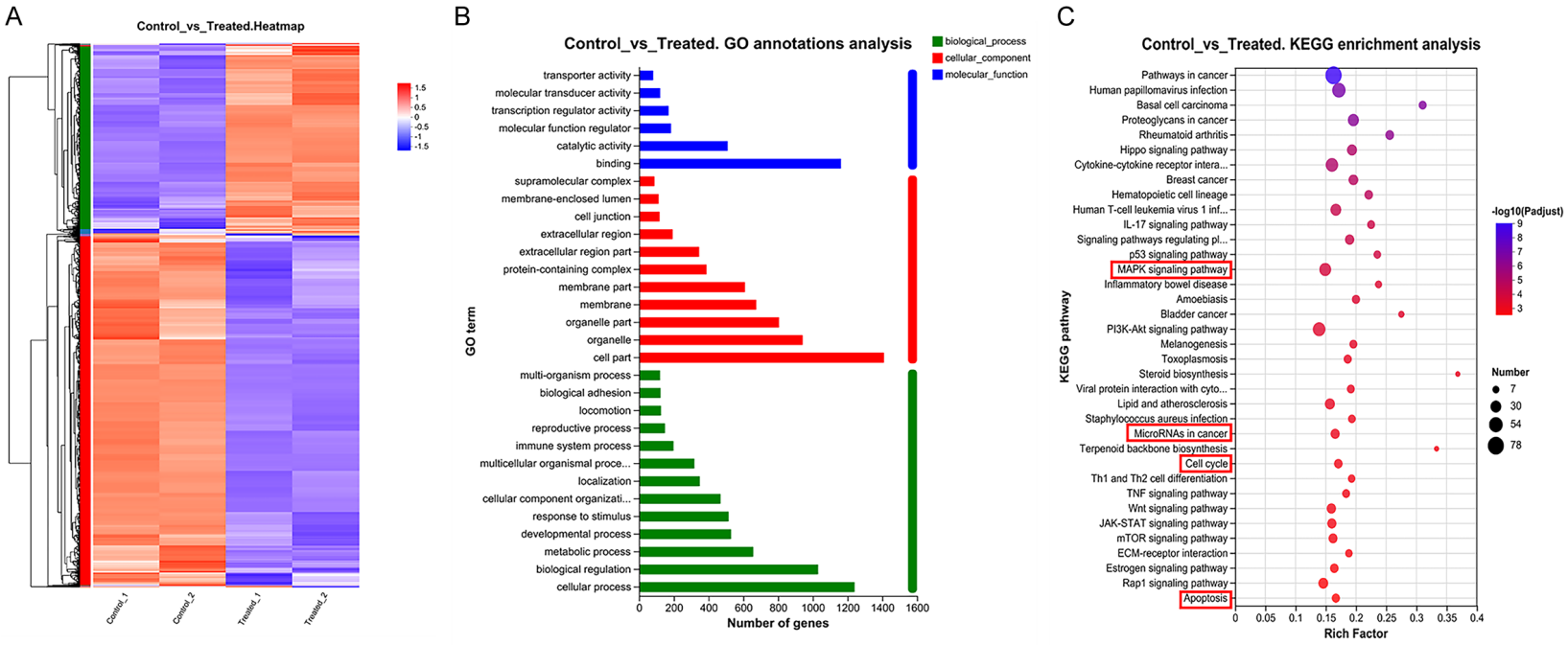

Figure 2. The analysis of DEGs induced by isoliensinine in HSC-3 cells. The DEGs induced by isoliensinine in HSC-3 cells are shown by clustering analysis; red indicates high expression, while blue indicates low expression (A). The GO annotation analysis (B) and the KEGG enrichment (C) analysis of DEGs. The vertical axis represents the GO terms or KEGG pathways, whereas the horizontal axis represents the number of genes or the rich factor.

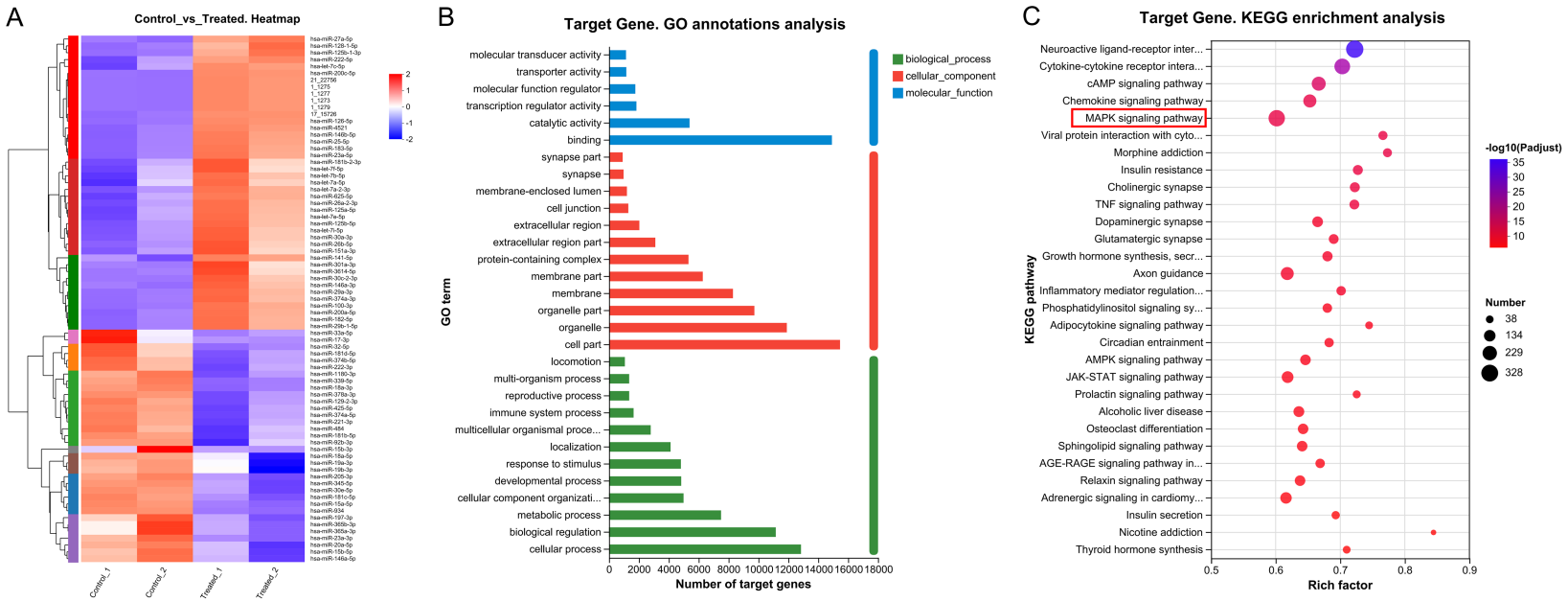

Figure 3. The effects of isoliensinine on miRNA expression in HSC-3 cells. The DEMs induced by isoliensinine in HSC-3 cells are shown by clustering analysis (A). GO annotation analysis (B) and KEGG enrichment analysis (C) of the target genes of the DEMs.

MAPK signaling pathway. To validate this prediction, the expression of key molecules in the MAPK pathway was further detected at the protein level. Western blot analysis of HSC-3 and HSC-4 cells treated with isoliensinine for 24 h revealed that isoliensinine significantly increased the levels of p-SAPK/JNK in the MAPK/JNK pathway and p-p38 in the MAPK/p38 pathway, while inhibiting the expression of p-ERK1/2 in the MAPK/ERK pathway (**Figure 4A-D**). These findings suggest that the MAPK signaling pathway is associated with the antiproliferative effect of isoliensinine on OSCC cells.

Isoliensinine arrests the cell cycle of OSCC cells at G2 phase

KEGG analysis of the DEGs indicated that the isoliensinine-mediated inhibition of HSC-3 cell proliferation was associated with cell cycle regulation. To investigate the molecular mechanism, the cell cycle distribution was analyzed by FCM with PI staining in HSC-3 and HSC-4 cells treated with isoliensinine for 12 h. The results revealed that the cell cycle was significantly arrested in G2 phase (**Figure 5A-D**). After treatment with 0, 20, 40, or 80 μM isoliensinine, the percentages of HSC-3 cells in G2 phase were (19.86±1.74)%, (26.29±0.52)%, (43.08±1.12)%, and (67.69±2.18)%, respectively, and those of the HSC-4 cells were (15.68±0.71)%, (21.61±0.82)%, (31.94±0.27)%, and (25.98±1.49)%, respectively.

To further elucidate the driving factors of G2 phase arrest, key regulatory molecules of the G2/M checkpoint were detected at the protein level. The Western blot results revealed that after 24 h of isoliensinine treatment, the levels of p-cdc25C and p-cdc2 increased in HSC-3 and HSC-4 cells, while Cyclin B1 expression was downregulated (**Figure 5E-H**). These results further confirmed that isoliensinine inhibits OSCC cell proliferation by arresting the cell cycle at the G2 phase.

Isoliensinine induces OSCC apoptosis

RNA-seq analysis demonstrated that the activation of apoptotic pathways constitutes a key mechanism underlying the antiproliferative effects of isoliensinine in HSC-3 cells. To probe the mechanism of by which isoliensinine induces OSCC cell death, HSC-3 and HSC-4 cells were stained with Annexin V-FITC/PI fluorescence after treatment with isoliensinine for 24 h. The FCM detection results indicated that isoliensinine induces OSCC apoptosis (**Figure 6A-D**). After treatment with 0, 20, 40, or 80 μM isoliensinine, the percentages of apoptotic HSC-3 cells were (2.79±1.88)%, (25.55±1.62)%, (40.37±0.45)%, and (91.04±6.61)%, respectively, and those of the HSC-4 cells were (2.27±0.43)%, (11.69±0.42)%, (21.85±0.92)%, and (64.75±1.13)%, respectively.

Furthermore, Western blot was performed to measure the expression levels of apoptosis-associated proteins. The results indicated that isoliensinine could upregulate the expression of cleaved caspase-9/-3 and cleaved PARP in HSC-3 and HSC-4 cells (**Figure 6E-H**). These results further confirmed isoliensinine inhibits OSCC cell proliferation by inducing apoptosis.

Isoliensinine triggers apoptosis in OSCC via the mitochondrial pathway

A decrease of the MMP is a significant event in the early stage of apoptosis. Treated with isoliensinine for 24 h, JC-1 staining followed by FCM analysis revealed a significant increase in the proportion of cells exhibiting decreased MMP in HSC-3 and HSC-4 cell lines (**Figure 7A-D**). Compared with the control group, after treatment with 80 μM isoliensinine, this proportion increased from (2.97±0.21)% to (91.31±1.91)% in HSC-3 and from (4.16±0.28)% to (64.43±1.00)% in HSC-4 cells.

The stability of the MMP is regulated by Bcl-2 family related proteins in the mitochondrial pathway. After being treated with isoliensinine for 24 h, the expression of Bcl-2 family proteins in HSC-3 and HSC-4 cells was detected via Western blot. The results demonstrate that isoliensinine upregulate the expression of the pro-apoptotic protein Bax and downregulate the expression of the anti-apoptotic protein Bcl-2 (**Figure 7E-H**). These results further confirmed that isoliensinine induces OSCC apoptosis through the mitochondrial pathway.

ROS participate in the induction of apoptosis by isoliensinine in OSCC cells

As triggers for the mitochondrial pathway, ROS can induce variations in the localization and expression levels of Bcl-2 family proteins, and

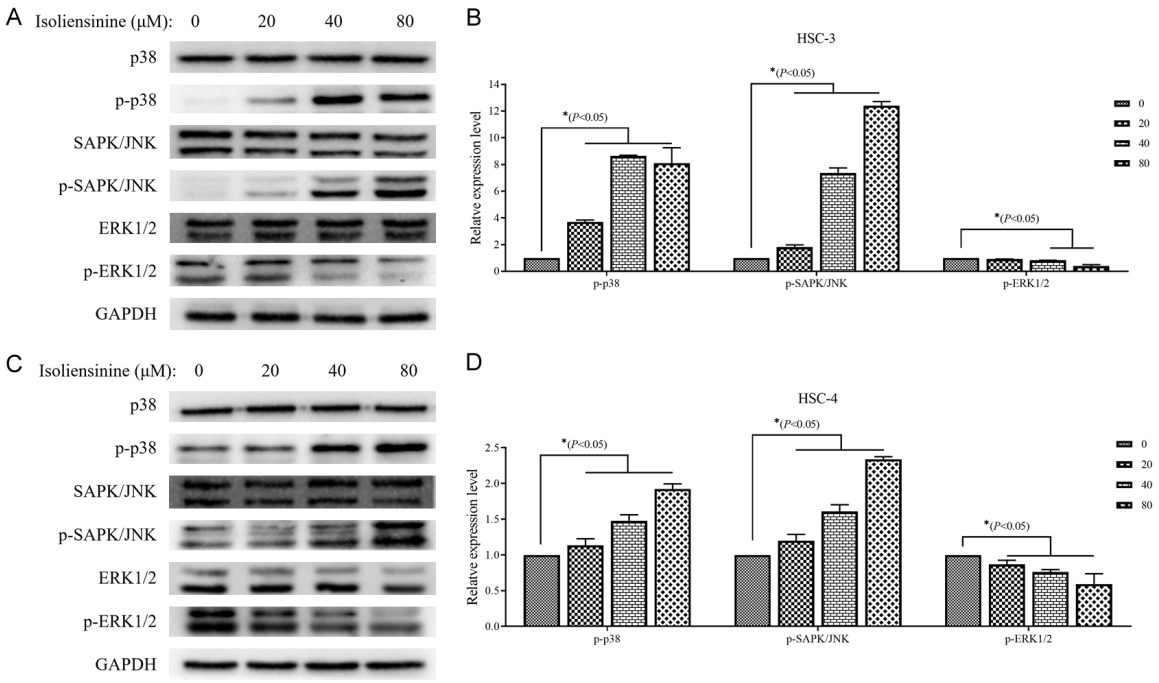

Figure 4. The effect of isoliensinine on the MAPK signaling pathway. After being treated with isoliensinine for 24 h, Western blot was employed for assessing the expression levels of MAPK signaling pathway-associated proteins in HSC-3 cells (A) and HSC-4 cells (C). The differential expression levels of MAPK signaling pathway-related proteins in HSC-3 cells (B) and HSC-4 cells (D) were analyzed statistically using GraphPad Prism 10.0 software. Data are expressed as mean ± SD (n = 3). Statistical significance was determined by one-way ANOVA followed by Dunnett's post-hoc test, with $*P < 0.05$ considered significant compared to the control group (0 μM isoliensinine).

promote apoptosis. Following 12 h of isoliensinine treatment, OSCC cells were loaded with DCFH-DA. FCM analysis revealed a marked increase in DCF fluorescence in HSC-3 and HSC-4 cells, confirming that isoliensinine enhances ROS production (**Figure 8A-D**). Compared with those in the 0 μM isoliensinine group, after treatment with 80 μM isoliensinine, the ROS levels in HSC-3 cells increased from (3.33±0.13)% to (37.28±0.33)%, and in HSC-4 cells increased from (3.46±0.45)% to (17.31±0.24)%. These results indicated that isoliensinine might induce OSCC apoptosis through the ROS-mediated mitochondrial pathway.

Discussion

The dibenzylidene isoquinoline alkaloids abundant in lotus germ, including isoliensinine, liensinine, and neferine, have been demonstrated to possess broad-spectrum antitumor activity. Despite structural similarity, their biological activities exhibit differences across various cancers [15]. For instance, in breast cancer studies, isoliensinine demonstrated stronger proliferation-inhibiting capabilities than liensinine and neferine [14]. In lung and liver cancer research, neferine has been extensively studied due to its potent induction of autophagy and apoptosis [16, 17]. However, compared with the relatively well-studied neferine, far less is known about the pharmacological effects and mechanisms of isoliensinine, particularly in OSCC. This study demonstrated that isoliensinine effectively inhibits the proliferation of OSCC cells in a time- and concentration-dependent manner. This finding not only aligns with previous conclusions regarding the broad-spectrum antitumor activity of this compound class but also highlights its research innovation in the specific context of OSCC.

Increasing ROS levels within cancer cells has been identified as an effective strategy for cancer treatment [18]. Isoliensinine has been demonstrated to induce cell death in breast and colorectal cancer by increasing intracellular ROS levels [14, 19]. In this study, the results of DCFH-DA fluorescence staining revealed that isoliensinine can increase ROS levels in the OSCC cells. ROS-induced apoptosis is closely

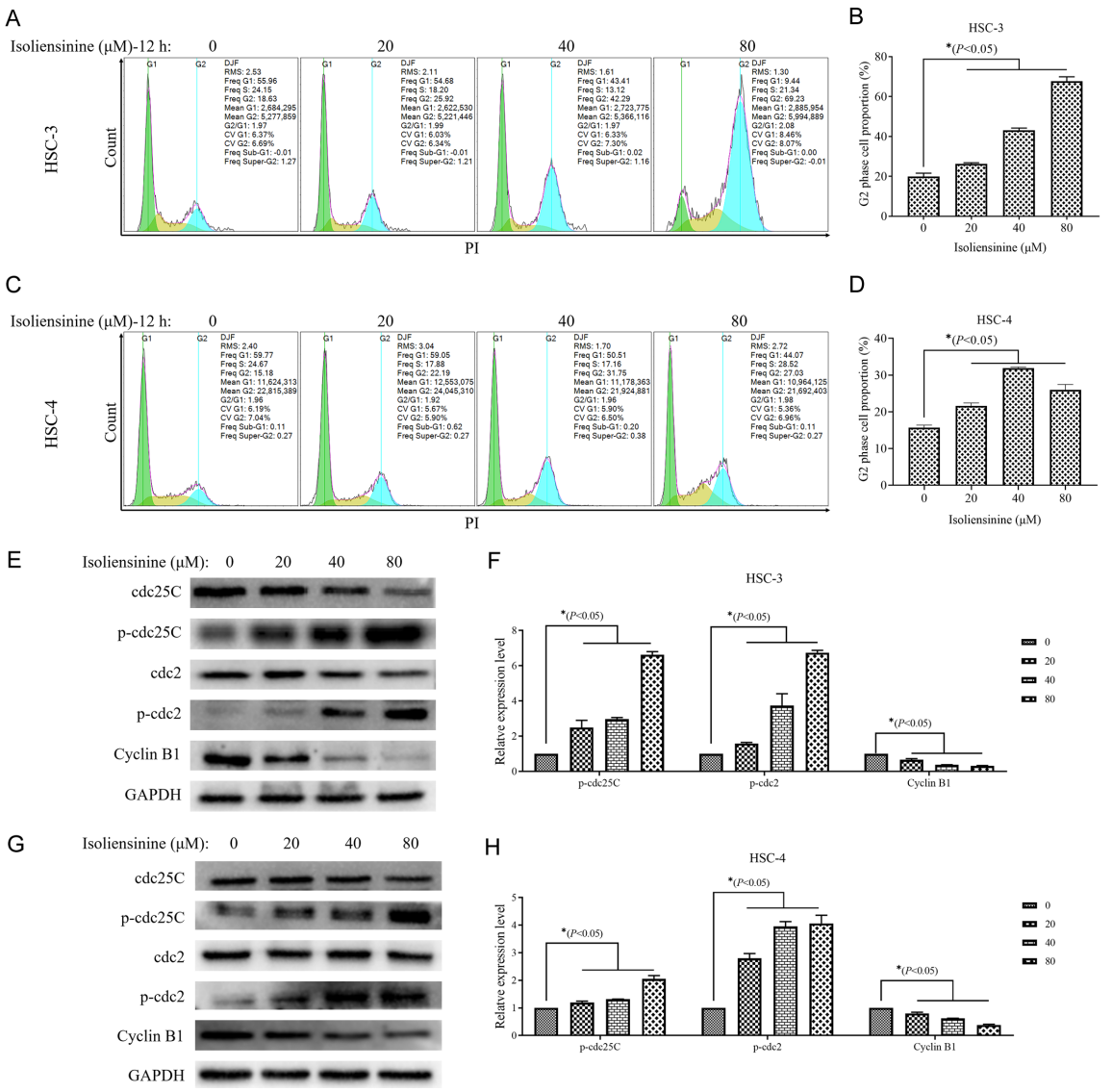

Figure 5. The effect of isoliensinine on OSCC cell cycle. After being treated with isoliensinine for 12 h, HSC-3 cells (A) and HSC-4 cells (C) stained with PI were collected by FCM for cell cycle distribution analysis. GraphPad Prism 10.0 software was adopted to statistically analyze the proportions of HSC-3 cells (B) and HSC-4 cells (D) in the G2 phase. After being treated with isoliensinine for 24 h, Western blot was served as assessing the expression level of cyclin in HSC-3 cells (E) and HSC-4 cells (G). The differences of cyclin expression in HSC-3 cells (F) and HSC-4 cells (H) were statistically analyzed by GraphPad Prism 10.0 software. Data are expressed as mean ± SD (n = 3). Statistical significance was determined by one-way ANOVA followed by Dunnett's post-hoc test, with $*P < 0.05$ considered significant compared to the control group (0 μM isoliensinine).

associated with mitochondrial outer membrane permeability, a process primarily regulated by the Bcl-2 protein family, in which Bax plays a central role [20]. Studies have shown that ROS can promote the translocation of Bax to the mitochondrial outer membrane, whereas the anti-apoptotic protein Bcl-2 directly antagonizes the pro-apoptotic function of Bax by forming heterodimers with it, thereby maintaining mitochondrial membrane stability [21]. We found that isoliensinine significantly increased the expression of Bax, while decreasing the expression of Bcl-2 in OSCC cells. Furthermore, it reduced the MMP, upregulated cleaved caspase-9/-3 and cleaved PARP, and ultimately induced apoptosis.

MAPK serves as a central hub for various signaling pathways and plays crucial roles in cell growth, development, and death. Excessive

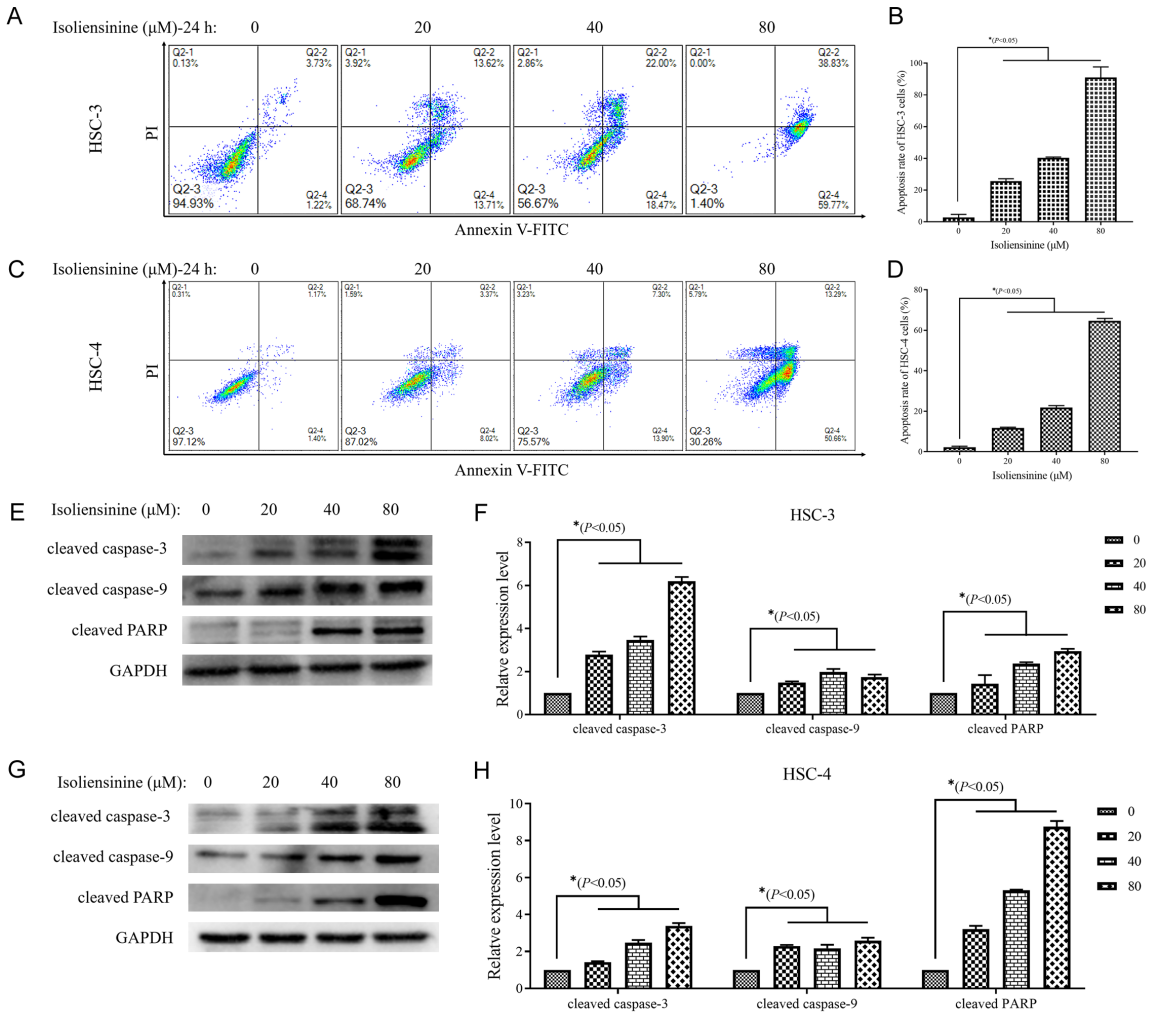

Figure 6. Isoliensinine induces apoptosis in OSCC cells. After treatment with isoliensinine for 24 h, HSC-3 cells (A) and HSC-4 cells (C) stained with Annexin V-FITC/PI were subjected to FCM for apoptosis analysis. GraphPad Prism 10.0 software was performed to statistically analyze the proportions of apoptotic HSC-3 cells (B) and HSC-4 cells (D). Western blot was adopted to assess the expression levels of apoptosis-associated proteins in HSC-3 cells (E) and HSC-4 cells (G). The differences of apoptosis-associated protein expression in HSC-3 cells (F) and HSC-4 cells (H) were statistically analyzed by GraphPad Prism 10.0 software. Data are expressed as mean ± SD (n = 3). Statistical significance was determined by one-way ANOVA followed by Dunnett's post-hoc test, with $*P < 0.05$ considered significant compared to the control group (0 μM isoliensinine).

activation of the MAPK/ERK signaling pathway has been found to promote tumor initiation and progression [22]. The MAPK/p38 and MAPK/JNK signaling pathways can participate in regulating the death receptor pathway and mitochondrial pathway through transcriptional regulation and posttranscriptional modification and upregulate the expression of p53, TNF-α, and Bcl-2 family proapoptotic proteins to promote apoptosis [23]. Isoliensinine can activate the p38 and JNK signaling pathways to induce apoptosis in breast cancer cells [14]. In line with prior research, our findings suggest that isoliensinine can increase the expression of p-SAPK/JNK and p-p38 in the OSCC cells. Notably, isoliensinine also appears to reduce the expression of p-ERK1/2 in OSCC cells. These studies suggest that isoliensinine could effectively induce apoptosis in OSCC cells by activating the MAPK signaling pathway.

It is reported that the MAPK signaling pathway is implicated in governing the cell cycle by modulating the activity and expression of diverse cell cycle-associated proteins, while also impacting the activity of transcription factors

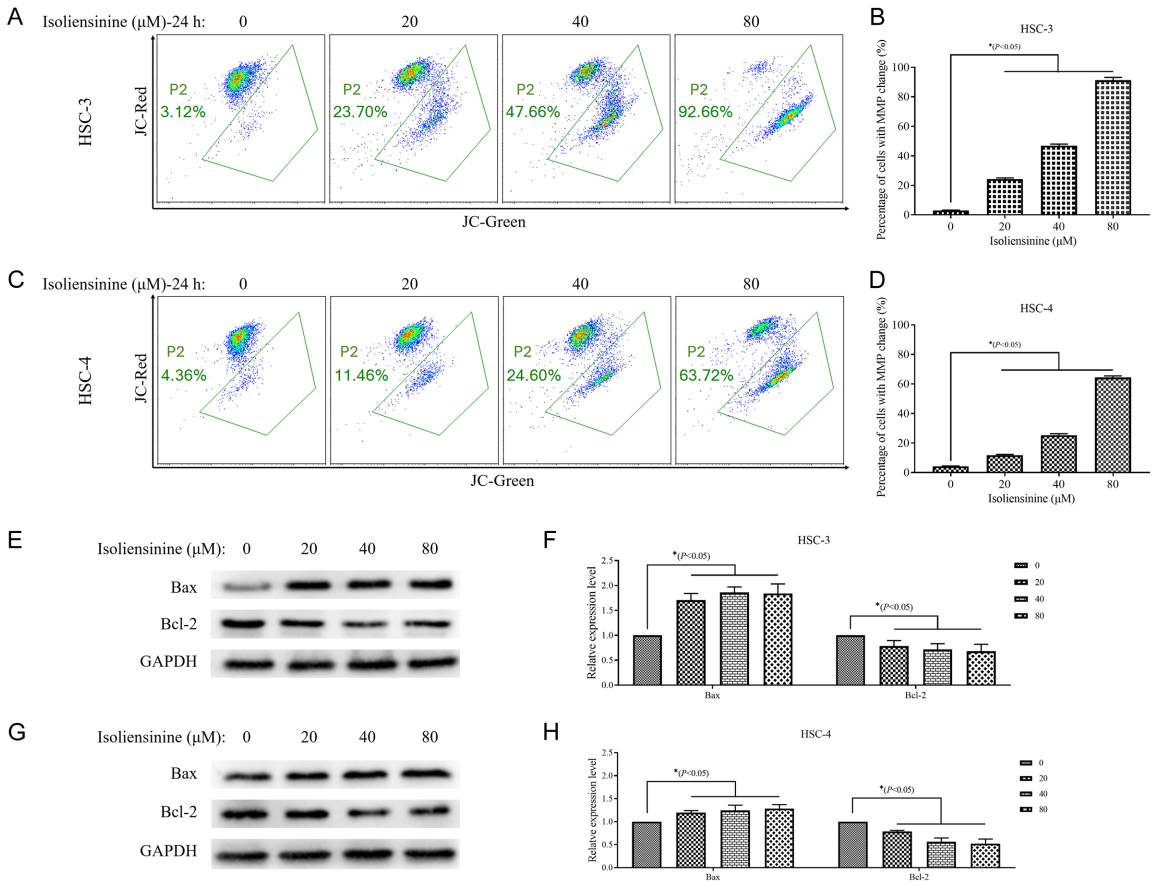

Figure 7. The effect of isoliensinine on the mitochondrial pathway in OSCC cells. After 24 h of treatment with isoliensinine, changes in MMP levels in HSC-3 (A) and HSC-4 (C) cells were analyzed via FCM. Primary single-cell populations were delineated using FSC/SSC scatter plots to exclude debris interference. Background thresholds for JC-1 monomer (green fluorescence) and JC-1 aggregate (red fluorescence) channels were established using unstained samples. Based on the distribution of control cells in the fluorescence plot, irregular polygonal gates were established to identify and delineate the P2 subpopulation exhibiting enhanced green fluorescence and reduced red fluorescence, representing cells with decreased MMP. A unified gating strategy was applied across all samples to determine the percentage of cells with reduced MMP in each treatment group. GraphPad Prism 10.0 software was applied to statistically analyze the percentage of cells with MMP in HSC-3 cells (B) and HSC-4 cells (D). Western blot was adopted to assess the expression levels of mitochondrial pathway-associated proteins in HSC-3 cells (E) and HSC-4 cells (G). The differences of the mitochondrial pathway-associated protein expression in HSC-3 cells (F) and HSC-4 cells (H) were statistically analyzed by GraphPad Prism 10.0 software. Data are expressed as mean ± SD (n = 3). Statistical significance was determined by one-way ANOVA followed by Dunnett's post-hoc test, with $*P < 0.05$ considered significant compared to the control group (0 μM isoliensinine).

[24]. The results of fluorescence staining with PI revealed that isoliensinine induces G2 phase arrest in OSCC cells. The cyclical progression of cells is tightly modulated by a range of cyclins and cyclin-dependent kinases (CDKs). The G2 phase is regulated mainly by cdc25C and CDK1 (cdc2). Cdc25C has phosphatase activity, which plays a pivotal role in the dephosphorylation of p-cdc2 in the inactivated state [25]. Dephosphorylation of p-cdc2 can activate the cdc2/cyclin B complex and promote cell entry into the M phase from the G2 phase. Our results demonstrated that isoliensinine could upregulate the expression of p-cdc25C and p-cdc2 in OSCC cells.

Phytochemicals have been shown to inhibit tumor cell proliferation by regulating miRNAs, which are crucial in tumor development [26, 27]. Compared with miRNA mimics or inhibitors, phytochemicals can simultaneously the expression of multiple miRNAs [28]. This makes them highly attractive for the biotreatment of tumors caused by multiple gene dysregula-

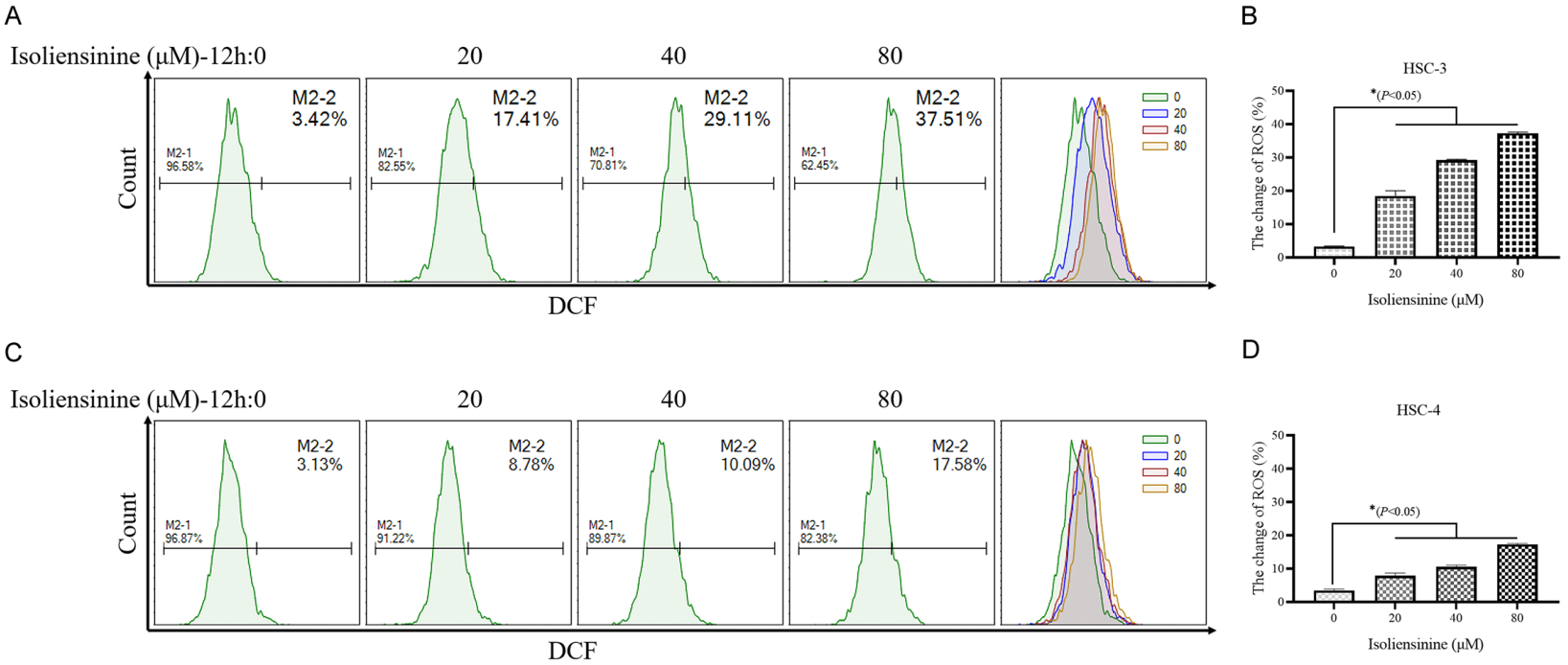

Figure 8. The effect of isoliensinine on intracellular ROS levels in OSCC cells. After being treated with isoliensinine for 12 h, HSC-3 cells (A) and HSC-4 cells (C) stained with a DCFH-DA probe were detected by FCM to analyze the change of intracellular ROS. GraphPad Prism 10.0 software was applied to statistically analyze the change of ROS in HSC-3 cells (B) and HSC-4 cells (D). Data are expressed as mean ± SD (n = 3). Statistical significance was determined by one-way ANOVA followed by Dunnett's post-hoc test, with $*P < 0.05$ considered significant compared to the control group (0 μM isoliensinine).

tions. KEGG enrichment analysis of DEGs induced by isoliensinine in HSC-3 cells revealed that isoliensinine may regulate miRNA expression in cancer. Notably, the regulatory effects of isoliensinine on tumor-related miRNAs, particularly in OSCC, remain unreported to date. On the basis of these findings, we further conducted small RNA-seq analysis and found that 77 miRNAs whose expression significantly differed were induced by isoliensinine in HSC-3 cells. These miRNAs with significant expression differences may be potential targets by which isoliensinine inhibits OSCC cell proliferation. GO and KEGG analyses revealed that the target genes of these miRNAs whose expression significantly differed were associated with cellular transcriptional regulatory activity, membrane components, and signaling pathways such as the MAPK and TNF pathways. These results align with the GO and KEGG analysis results of DEGs induced by isoliensinine, suggesting that isoliensinine may impact gene expression by modulating miRNA expression, thereby exerting an inhibitory effect on OSCC cell proliferation.

Here, it must be acknowledged that there are limitations in this study, and follow-up research is needed to address them. Firstly, the current findings are based on limited cell line experiments and have not yet been validated in animal models. To comprehensively evaluate its antitumor potential and translational prospects, subsequent studies should incorporate more representative cell lines and systematically validate its in vivo efficacy and safety through animal experiments. Secondly, it warrants further investigation whether isoliensinine exhibits a selective mechanism of action against cancer cells. This selectivity may stem from inherent differences between normal cells and cancer cells in the expression of relevant miRNAs and the regulation of MAPK signaling pathways [29]. In cancer cells, isoliensinine may induce stronger and sustained MAPK activation via miRNAs.

In fact, the clinical translation of isoliensinine still faces significant challenges, primarily stemming from its cytotoxic mechanism based on elevated ROS levels - while it can selectively target tumor cells undergoing metabolic stress, imprecise control may pose risks of oxidative damage to normal tissues [30]. Furthermore, constrained by the inherent limitations of natural alkaloid-based drugs, this compound generally exhibits issues such as low oral bioavailability, rapid systemic clearance, and insufficient tumor accumulation [31]. To overcome these limitations, a multidimensional development strategy is required: improving solubility, metabolic stability, and selectivity through rational structural modifications; and utilizing advanced delivery systems such as tumor-targeting nanocarriers to optimize biodistribution, promoting selective accumulation of the drug at tumor sites while reducing systemic exposure [32].

And we should recognize that combination therapy represents a key direction for enhancing the clinical applicability of isoliensinine. As elucidated in this study, its mechanism of action suggests that isoliensinine may exhibit synergistic potential with conventional therapies for OSCC across multiple pathways. For example, isoliensinine can significantly lower the apoptotic threshold of tumor cells by modulating apoptosis-related proteins. When combined with chemotherapeutic agents such as platinum-based drugs, 5-fluorouracil, or paclitaxel, the apoptotic signaling pathways induced by isoliensinine synergize with the DNA damage or microtubule disruption effects triggered by these chemotherapeutic drugs, thereby further promoting terminal apoptosis of tumor cells [33]. Moreover, since the MAPK pathway is a key downstream component of EGFR signaling, isoliensinine may act as a sensitizer to overcome resistance to EGFR-targeted drugs such as cetuximab [34].

Conclusion

In conclusion, our findings indicate that isoliensinine inhibits the proliferation of the OSCC cells in vitro. This inhibitory effect is associated with the differential expression of 1878 genes and 77 miRNAs, which can regulate cell signaling pathways such as the MAPK signaling pathway. Further experimental studies have demonstrated that isoliensinine exerts anti-OSCC effects by modulating the MAPK signaling pathway, triggering the ROS-mediated mitochondrial pathway and G2 phase arrest, ultimately culminating in apoptosis. Compared with existing research, this study not only provides a new direction for research on the antitumor mechanism of isoliensinine, but also establishes a

new theoretical framework for the use of the miRNA-MAPK regulatory network in OSCC treatment, providing an important theoretical basis and innovative ideas for the development of targeted treatment strategies based on natural compounds.

Acknowledgements

We acknowledge Professor Mingbo Wu from the State Key Laboratory of Biotherapy of Sichuan University for providing the human OSCC cell lines HSC-3 and HSC-4. The present study was supported by the Science and Technology Department of Sichuan Province (No. 2023NSFSC0725), the National Undergraduates Innovating Experimentation Project of China (No. 202413705028, No. 20251370-5003, No. 202513705007, No. 202513705-022), the Key Laboratory Project of Major Disease Target Discovery and Protein Drug Development at Sichuan Provincial Universities (No. 23LHNBZYB07), and the Research and Innovation Fund for Postgraduates of Chengdu Medical College (No. YCX2025-01-11).

Disclosure of conflict of interest

None.

Address correspondence to: Min-Hui Li and Ping Yang, Chengdu Medical College, No. 783, Xindu Avenue, Xindu District, Chengdu 610500, Sichuan, China. E-mail: liminhui@cmc.edu.cn (MHL); yangping@cmc.edu.cn (PY)

References

[1] Bray F, Laversanne M, Sung H, Ferlay J, Siegel RL, Soerjomataram I and Jemal A. Global cancer statistics 2022: GLOBOCAN estimates of incidence and mortality worldwide for 36 cancers in 185 countries. CA Cancer J Clin 2024; 74: 229-263.

[2] Chamoli A, Gosavi AS, Shirwadkar UP, Wangdale KV, Behera SK, Kurrey NK, Kalia K and Mandoli A. Overview of oral cavity squamous cell carcinoma: risk factors, mechanisms, and diagnostics. Oral Oncol 2021; 121: 105451.

[3] National Institutes of Health Cancer Stat Facts: Oral Cavity and Pharynx Cancer [April 2025]. Available from: https://seer.cancer.gov/statfacts/html/oralcav.html.

[4] Cramer JD, Burtness B, Le QT and Ferris RL. The changing therapeutic landscape of head and neck cancer. Nat Rev Clin Oncol 2019; 16: 669-683.

[5] Young K, Bulosan H, Kida CC, Bewley AF, Abouyared M and Birkeland AC. Stratification of surgical margin distances by the millimeter on local recurrence in oral cavity cancer: a systematic review and meta-analysis. Head Neck 2023; 45: 1305-1314.

[6] Imbesi Bellantoni M, Picciolo G, Pirrotta I, Irrera N, Vaccaro M, Vaccaro F, Squadrito F and Pallio G. Oral cavity squamous cell carcinoma: an update of the pharmacological treatment. Biomedicines 2023; 11: 1112.

[7] Parmar A, Macluskey M, Mc Goldrick N, Conway DI, Glenny AM, Clarkson JE, Worthington HV and Chan KK. Interventions for the treatment of oral cavity and oropharyngeal cancer: chemotherapy. Cochrane Database Syst Rev 2021; 12: CD006386.

[8] Atashi F, Vahed N, Emamverdizadeh P, Fattahi S and Paya L. Drug resistance against 5-fluorouracil and cisplatin in the treatment of head and neck squamous cell carcinoma: a systematic review. J Dent Res Dent Clin Dent Prospects 2021; 15: 219-225.

[9] Lee TY and Tseng YH. The potential of phytochemicals in oral cancer prevention and therapy: a review of the evidence. Biomolecules 2020; 10: 1150.

[10] Olofinsan K, Abrahamse H and George BP. Therapeutic role of alkaloids and alkaloid derivatives in cancer management. Molecules 2023; 28: 5578.

[11] Cheng Y, Li HL, Zhou ZW, Long HZ, Luo HY, Wen DD, Cheng L and Gao LC. Isoliensinine: a natural compound with “drug-like” potential. Front Pharmacol 2021; 12: 630385.

[12] Shu G, Yue L, Zhao W, Xu C, Yang J, Wang S and Yang X. Isoliensinine, a bioactive alkaloid derived from embryos of nelumbo nucifera, induces hepatocellular carcinoma cell apoptosis through suppression of NF-kappaB signaling. J Agric Food Chem 2015; 63: 8793-8803.

[13] Li HL, Cheng Y, Zhou ZW, Long HZ, Luo HY, Wen DD, Cheng L and Gao LC. Isoliensinine induces cervical cancer cell cycle arrest and apoptosis by inhibiting the AKT/GSK3alpha pathway. Oncol Lett 2022; 23: 8.

[14] Zhang X, Wang X, Wu T, Li B, Liu T, Wang R, Liu Q, Liu Z, Gong Y and Shao C. Isoliensinine induces apoptosis in triple-negative human breast cancer cells through ROS generation and p38 MAPK/JNK activation. Sci Rep 2015; 5: 12579.

[15] Manogaran P, Beeraka NM and Padma VV. The cytoprotective and anti-cancer potential of bisbenzylisoquinoline alkaloids from nelumbo nucifera. Curr Top Med Chem 2019; 19: 2940-2957.

[16] Zhong PC, Liu ZW, Xing QC, Chen J and Yang RP. Neferine inhibits the development of lung

cancer cells by downregulating TGF-beta to regulate MST1/ROS-induced pyroptosis. Kaohsiung J Med Sci 2023; 39: 1106-1118.
[17] Hu P, Wan P, Xu A, Yan B, Liu C, Xu Q, Wei Z, Xu J, Liu S, Yang G and Pan Y. Neferine, a novel ROCK1-targeting inhibitor, blocks EMT process and induces apoptosis in non-small cell lung cancer. J Cancer Res Clin Oncol 2023; 149: 553-566.
[18] Nakamura H and Takada K. Reactive oxygen species in cancer: current findings and future directions. Cancer Sci 2021; 112: 3945-3952.
[19] Manogaran P, Beeraka NM, Huang CY and Vijaya Padma V. Neferine and isoliensinine enhance 'intracellular uptake of cisplatin' and induce 'ROS-mediated apoptosis' in colorectal cancer cells - A comparative study. Food Chem Toxicol 2019; 132: 110652.
[20] Kalkavan H and Green DR. MOMP, cell suicide as a BCL-2 family business. Cell Death Differ 2018; 25: 46-55.
[21] Zhang A, Wang Y, Xue Q, Yao J, Chen L, Feng S, Shao J, Guo Z, Zhou B and Xie J. Polystyrene microplastics disrupt kidney organoid development via oxidative stress and Bcl-2/Bax/caspase pathway. Chem Biol Interact 2025; 419: 111642.
[22] Sugiura R, Satoh R and Takasaki T. ERK: a double-edged sword in cancer. ERK-dependent apoptosis as a potential therapeutic strategy for cancer. Cells 2021; 10: 2509.
[23] Yue J and Lopez JM. Understanding MAPK signaling pathways in apoptosis. Int J Mol Sci 2020; 21: 2346.
[24] Taylor WR and Stark GR. Regulation of the G2/M transition by p53. Oncogene 2001; 20: 1803-1815.
[25] Liu K, Zheng M, Lu R, Du J, Zhao Q, Li Z, Li Y and Zhang S. The role of CDC25C in cell cycle regulation and clinical cancer therapy: a systematic review. Cancer Cell Int 2020; 20: 213.
[26] Ghosh RD, Pattatheyil A and Roychoudhury S. Functional landscape of dysregulated micrornas in oral squamous cell carcinoma: clinical implications. Front Oncol 2020; 10: 619.
[27] Ruiz-Manriquez LM, Estrada-Meza C, Benavides-Aguilar JA, Ledesma-Pacheco SJ, Torres-Copado A, Serrano-Cano FI, Bandyopadhyay A, Pathak S, Chakraborty S, Srivastava A, Sharma A and Paul S. Phytochemicals mediated modulation of microRNAs and long non-coding RNAs in cancer prevention and therapy. Phytother Res 2022; 36: 705-729.
[28] Shoaib A, Tabish M, Ali S, Arafah A, Wahab S, Almarshad FM, Rashid S and Rehman MU. Dietary phytochemicals in cancer signalling pathways: role of miRNA targeting. Curr Med Chem 2021; 28: 8036-8067.
[29] Saliani M, Mirzaiebadizi A, Javadmanesh A, Siavoshi A and Ahmadian MR. KRAS-related long noncoding RNAs in human cancers. Cancer Gene Ther 2022; 29: 418-427.
[30] Iqbal MJ, Kabeer A, Abbas Z, Siddiqui HA, Calina D, Sharifi-Rad J and Cho WC. Interplay of oxidative stress, cellular communication and signaling pathways in cancer. Cell Commun Signal 2024; 22: 7.
[31] Yao M, Wu M, Yuan M, Wu M, Shen A, Chen Y, Lian D, Liu X and Peng J. Enhancing the therapeutic potential of isoliensinine for hypertension through PEG-PLGA nanoparticle delivery: a comprehensive in vivo and in vitro study. Biomed Pharmacother 2024; 174: 116541.
[32] Zhang HX, Lin LF, Liu YL and Li H. Research progress in anti-tumor activity and nano-drug delivery system of piperlongumine. Zhongguo Zhong Yao Za Zhi 2024; 49: 2117-2127.
[33] Guler EM, Bozali K, Huseyinbas O, Celikten M and Kocyigit A. Combination of 5-fluorouracil and thymoquinone for enhanced cytotoxicity, genotoxicity and apoptosis in colorectal cancer: in vitro and in vivo studies. J Biochem Mol Toxicol 2025; 39: e70276.
[34] Zhao Z, He J, Qiu S, Wang L, Huangfu S, Hu Y, Wu Q, Yang Y, Li X, Huang M, Liu S, Guan H, Chen Z, Zhang X, Zhang Y, Ding H, Zhao X, Xiao G, Pan Y, Liu T, Wu Y and Pan J. Targeting PLK1-CBX8-GPX4 axis overcomes BRAF/EGFR inhibitor resistance in BRAFV600E colorectal cancer via ferroptosis. Nat Commun 2025; 16: 3605.